Preprints.org

Article

Not peer-reviewed version

Activation Mechanism of Water Dissociation for Catalytic Hydrogen Production: Insights from First-Principles Molecular Dynamics Simulation

Tingting Liu , Xinglong Pan , Yanbiao Wang *

Posted Date: 18 February 2025

doi: 10.20944/preprints202502.1433.v1

Keywords: Water Dissociation; First-principles Molecular Dynamics; Catalysis; Infrared Spectrum of Vibration; Frontier Orbitals; Resonance Absorption of Heat

Preprints.org is a free multidisciplinary platform providing preprint service that is dedicated to making early versions of research outputs permanently available and citable. Preprints posted at Preprints.org appear in Web of Science, Crossref, Google Scholar, Scilit, Europe PMC.

Copyright: This open access article is published under a Creative Commons CC BY 4.0 license, which permit the free download, distribution, and reuse, provided that the author and preprint are cited in any reuse.

Preprints.org (www.preprints.org) | NOT PEER-REVIEWED | Posted: 18 February 2025 doi:10.20944/preprints202502.1433.v1

Disclaimer/Publisher's Note: The statements, opinions, and data contained in all publications are solely those of the individual author(s) and contributor(s) and not of MDPI and/or the editor(s). MDPI and/or the editor(s) disclaim responsibility for any injury to people or property resulting from any ideas, methods, instructions, or products referred to in the content.

Article

Activation Mechanism of Water Dissociation for Catalytic Hydrogen Production: Insights from First-Principles Molecular Dynamics Simulation

Tingting Liu [1], Xinglong Pan [2] and Yanbiao Wang [1,3,*]

[1] Department of Fundamental Courses, Wuxi Institute of Technology, Wuxi 214121, China
[2] School of Mechanical Technology, Wuxi Institute of Technology, Wuxi 214121, China
[3] Southeast University, Nanjing 211189, China
* Correspondence: 770720786@qq.com

Abstract: One of the most challenging issues in catalytic water dissociation hydrogen production technology is understanding the activation mechanism of water. To gain insights into this process, a first-principles molecular dynamics method was used to simulate the catalytic dissociation of H2O on 88 alloy catalysts. The study's results revealed that a larger red shift of the center of the v1 and v3 modes of adsorbed H2O corresponds to a lower dissociation temperature. The resonance absorption of heat from water molecules by the frontier electron promotes the dissociation reaction. Comparing the frontier orbitals of precursors and intermediate states shows that the number of involved frontier orbitals significantly influences the catalytic reaction.

Keywords: water dissociation; first-principles molecular dynamics; catalysis

1. Introduction

Hydrogen, a clean and renewable energy source, has the potential to address global warming, environmental pollution, and the fossil energy crisis [1–3]. The overall reaction for hydrogen production by water splitting is an "uphill reaction" with an unfavorable positive free Gibbs energy of ΔG_o = 237.13 kJ/mol^{-1}, and it usually cannot occur spontaneously due to a barrier. Catalysts with electronic and optical properties that can be tailored to specific dimensions, shapes, and compositions can reduce the energy barriers associated with chemical reactions, thereby facilitating their occurrence [4]. Since the initial report in 1972 demonstrating photoelectrochemical water splitting under UV irradiation with an n-type TiO_2 photoanode and a Pt cathode for H2 evolution (the Honda-Fujishima effect) [5], there has been a vast quantity of research articles and reviews focusing on various materials for photocatalytic water splitting [*6–21*].

The dissociation of water can be achieved by electronic excitations [22,23] or by vibrational excitation [24,25]. The water molecule exhibits three distinct vibrational normal modes: bending (v_2), symmetric (v_1), and antisymmetric (v_3) stretching modes. The two stretching modes are strongly coupled (Darling–Dennison coupling) due to the close vibrational frequencies and anharmonicity, while the coupling between the bending mode and the stretching motion is weak [26,27]. Polanyi's rule posits that a "late" barrier is more readily surmounted by vibrational excitation, whereas an "earlier" barrier is more readily overcome by translational energy. This is based on the observation that the "promoting coordinate" coincides with the reaction coordinate near the transition state in each case [28]. The dissociative chemisorption of H_2O has a late barrier, where the bond cleavage occurs after the molecule adsorbs on the surface. Consequently, vibrational excitation of H_2O may have a significant impact on reactivity. Vibrationally excited molecular hydrogen has been observed in the dense photodominated regions [29]. Experimentalists have previously reported that in the presence of a laser field, vibrational excitation increases the reactivity of unimolecular and

© 2025 by the author(s). Distributed under a Creative Commons CC BY license.

Preprints.org (www.preprints.org) | NOT PEER-REVIEWED | Posted: 18 February 2025 doi:10.20944/preprints202502.1433.v1

bimolecular reactions more than translational and rotational excitation [30,31]. Theoretical studies of water dissociative chemisorption have predicted that water on Cu(111) and Ni(111) exhibits strong mode specificity, bond selectivity, and steric effects [32–35]. In a pioneering study, Zhang *et al.* employed full-dimensional quantum dynamics to investigate the dissociative chemisorption of H_2O on rigid Cu(111). Their findings revealed that the excitations in vibrational modes of H_2O play a more pivotal role than increasing the translational energy in promoting the reaction. Moreover, they demonstrated that the enhancement of the excitation in asymmetric stretching is the most pronounced [36]. The influence of alloying on mode-selectivity in H_2O dissociation on Ni(100), Ni(110), Ni(111) and Cu/Ni bimetallic surfaces has been investigated by Tiwari et al. The authors employed a fully quantum approach based on the reaction path Hamiltonian, which revealed that mode specificity of H_2O dissociation was observed on all the surfaces. This invariably suggested that the vibrational excitation resulted in a significant enhancement in reactivity for all systems [37,38]. These conclusions are consistent with those of quantum state-resolved molecular beam experiments on the dissociation of heavy water on Ni (111) [39]. The vibrational enhancement of reactivity can be understood by the sudden vector projection (SVP) model, and the enhancement of reactivity by Polanyi's rule mode reflects its coupling with the reaction coordinate at the transition state [40,41]. Indeed, Kim *et al.* have successfully manipulated the state-selective dissociation of a single water molecule using inelastic tunneling electrons with a low-temperature scanning tunnelling microscope. This process results in the dissociation of water into hydroxyl by the excitation of the vibrational state of the stretching modes and into atomic oxygen by the excitation of the electronic state [42]. Additionally, vibrationally excited hydrolysis dissociation experiments are an effective means of measuring hydrolysis dissociation thresholds. For instance, Maksyutenko *et al.* accurately determined the value of the first dissociation threshold of water, $D_0 = 41145.94 \pm 0.15$ cm^{-1}, from the onset of the dissociative continuum in triple-resonance spectra [43].

The atomic-scale insights into the interactions of water molecules with catalysts have long been recognized as essential, given the fundamental role of these interactions in the elementary process of hydrogen generation. The theoretical calculations based on density functional theory (DFT) have been employed to elucidate the mechanism of water interaction with metal surfaces at the molecular level [33]. Despite substantial efforts in both experimental and theoretical studies, to date only a few works have been published on the role of chemical shifts in the infrared spectra of water molecules when adsorbed on catalysts in characterizing the reactivity of water molecules. Since vibrational spectroscopy can provide information on the structure and the bonding of the molecules, the correlation between reactivity and chemical shift in the infrared vibrational spectra of H_2O on the $Cu_{(10-n)}Pt_n$ and $Cu_{(9-n)}Pd_n$ alloy catalysts has been studied [44,45]. In these studies, we introduced the concept of the center of the v_1 and v_3 modes (the center of the v_1 and v_3 modes = (v_1 ×intensity of v_1 + v_3×intensity of v_3)/ (intensity of v_1 + intensity of v_3)) is used to characterize the reactivity of water molecules due to the strong coupling of the two stretching modes of H_2O with the reaction coordinate. The results indicated that the dissociation barrier of H_2O is closely dependent on the red shift of the center of the v_1 and v_3 modes of H_2O adsorbed. The larger the red shift of the center of the v_1 and v_3 modes is, the lower the corresponding barrier is. It is therefore hypothesized that the red shift of the center due to the adsorption of water molecules on the catalyst can be used to characterize the activation properties of the catalysts. This study examines the chemical shifts observed in the infrared vibrational spectra of H_2O adsorbed on 88 alloy clusters, with the objective of testing this hypothesis and developing a predictive understanding of the activity of the catalysts.

2. Computational Details

In this study, we optimized the structures of catalysts using the generalized gradient approximation (GGA) with the Perdew-Burke-Ernzerhof (PBE) functional [46] and a density functional theory (DFT)-based relativistic semicore pseudo-potential (DSPP) [47]. Subsequently, infrared spectra were calculated. In order to investigate the effect of the heat of adsorption reaction of water molecules, we selected the NVE ensemble and conducted a first-principles molecular

Preprints.org (www.preprints.org) | NOT PEER-REVIEWED | Posted: 18 February 2025 doi:10.20944/preprints202502.1433.v1

dynamics simulation of the catalytic dissociation of H_2O molecules at temperatures ranging from 0 to 1500 K, with a temperature step of 100 K. The time step and the total simulation time were 1 fs and 5 ps, respectively. All pertinent details have been provided in the supplementary material.

3. Results and Discussions

3.1. Identification and Construction of Research Subjects

The adsorption behavior of H_2O on the first 75 single atoms in the periodic table was initially investigated. Three cases of being positively charged, uncharged, and negatively charged were considered separately, as illustrated in Figure 1. The red shifts of the center of the v_1 and v_3 modes of H_2O adsorbed on single atoms were then plotted in relation to that of the isolated H_2O in an electrically neutral state. It is evident that the red shift of the center of the stretching vibration modes of H_2O adsorbed on the single atom carrying a negative charge is considerably larger than that of the other two cases. This phenomenon exhibits a certain periodic behavior that is closely dependent on the nature of the elements. The reason why inert elements exhibit high activity in negative charge is that their high stability makes it easier for electrons to transfer to water molecules, thereby leaving the water molecules in a more active state. Consequently, the extent of the red shift of the center of the v_1 and v_3 modes of H_2O adsorbed on inert elements is comparable to that observed when the water molecule carries a direct negative charge.

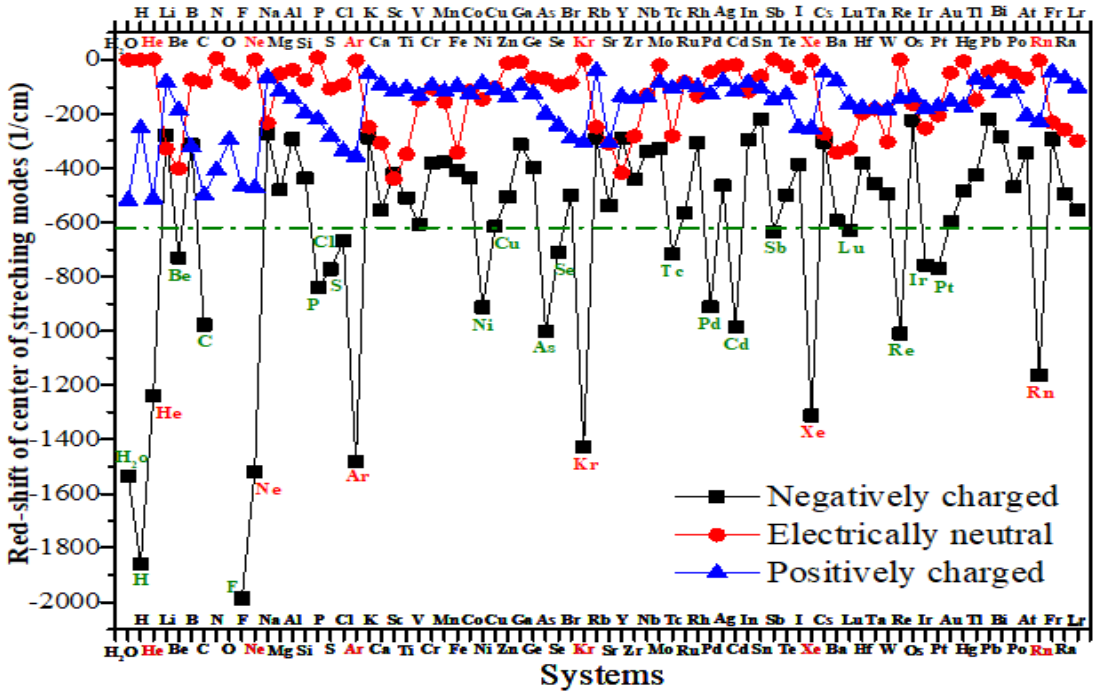

Figure 1. The red shifts of the centers of v_1 and v_3 modes of H_2O adsorbed on the first 75 single atoms in the periodic table relative to isolated electrically neutral H_2O are presented. The black squares, red circles, and blue triangles represent negative charge, no charge, and a positive charge, respectively.

The catalytic dissociation of water is typically achieved through the use of Cu and Pt metal surfaces [9,*38*]. The red shift of the center of the stretching (v_1 and v_3) modes of H_2O adsorbed on the negatively charged Cu atom is 615 1/cm, as illustrated by the green dash-dotted line in Figure 1. The construction of 24 diatomic alloy clusters, 30 triatomic alloy clusters, and 34 tetraatomic alloy clusters, based mainly on Pt, was carried out using sodium elements representing alkali metals and elements with redshift scales exceeding that of copper, as shown in Table 1. Subsequently, the catalytic dissociation of H_2O molecules over the aforementioned catalysts was simulated within a temperature range of 50–1500 K.

Preprints.org (www.preprints.org) | NOT PEER-REVIEWED | Posted: 18 February 2025 doi:10.20944/preprints202502.1433.v1

Table 1. 24 diatomic, 30 triatomic, and 34 tetraatomic clusters were constructed and listed below.

Diatomic clusters 24	**BePt**	**CPt**	**NPt**	**FPt**	**NaPt**	**PPt**
	NiPt	**Cu_2**	**CuPt**	**AsPt**	**SrCd**	**SrRe**
	SrPt	**TcPt**	**PdPt**	**Cd_2**	**CdRe**	**CdPt**
	SbPt	**Re_2**	**RePt**	**IrPt**	**Pt_2**	**PtAu**
Triatomic clusters 30	Be_2Pt	C_2Pt	N_2Pt	F_2Pt	Na_2Pt	$NaPt_2$
	P_2Pt	Ni_2	Ni_2Pt	Cu_3	Cu_2Pt	As_2Pt
	Sr_2Cd	Sr_2Re	Sr_2Pt	$SrCd_2$	$SrRe_2$	$SrPt_2$
	Tc_2Pt	Pd_2Pt	Cd_3	Cd_2Re	Cd_2Pt	$CdRe_2$
	Sb_2Pt	Re_3	Re_2Pt	Ir_2Pt	Pt_3	$PtAu_2$
Tetraatomic clusters 34	Be_3Pt	C_3Pt	N_3Pt	F_3Pt	Na_4	Na_3Pt
	Na_2Pt_2	$NaPt_3$	P_3Pt	Ni_3Pt	$NiPt_3$	Cu_4
	Cu_3Pt	As_3Pt	Sr_4	Sr_3Cd	Sr_3Re	Sr_3Pt
	Sr_2Re_2	Sr_2Pt_2	$SrCd_3$	$SrRe_3$	$SrPt_3$	Tc_3Pt
	Pd_3Pt	Cd_4	Cd_3Re	Cd_3Pt	$CdRe_3$	Sb_3Pt
	Re_4	Re_3Pt	Ir_3Pt	Pt_4		

3.2. Dependence of Dissociation Temperature on Infrared Vibrational Spectra

The dependence of the catalytic dissociation temperature of water on the red shift of the center of the v_1 and v_3 modes of H_2O on different clusters is shown in Figure 2. For comparison, the red shift of the center of the v_1 and v_3 modes of H_2O is relative to the negatively charged isolated H_2O (ΔIR). For catalysts with a water dissociation temperature above 1500K, the dissociation temperatures are all marked as 1500K for ease of plotting. It is evident that clusters with less than 300 1/cm of ΔIR have high catalytic water dissociation activity, corresponding to a dissociation temperature of no more than 200K. For ΔIR is between 300 and 700 1/cm, except for Sr_3Pt and CuPt, these clusters still showed high catalytic activity with dissociation temperatures not higher than 600K. For the red shifts in the 700-1016 1/cm range, different catalysts showed significant variations in catalytic activity. Other catalysts corresponding to higher ΔIR showed no visible catalytic activity. The results here show that the red shift of the center of the v_1 and v_3 modes of H_2O, which takes into account the strong coupling of the two stretching modes [26,27], allows a good characterization of the catalytic reactivity of water molecules. Given that the dissociation of water on these catalysts occurs mainly through a late-barrier reaction, as shown in Figure S1, it is reasonable to expect the above results from the Polanyi's law and the Sudden Variation Vector Projection (SVP) model [39,40] as well. It is also consistent with the results observed by Tiwari's group in their work on vibrationally excited dissociation of water molecules on Ni surfaces, where the softening of symmetric stretching and bending modes suggests that the excitation of these modes would lead to a significant enhancement in reaction probabilities [37].

Preprints.org (www.preprints.org) | NOT PEER-REVIEWED | Posted: 18 February 2025 doi:10.20944/preprints202502.1433.v1

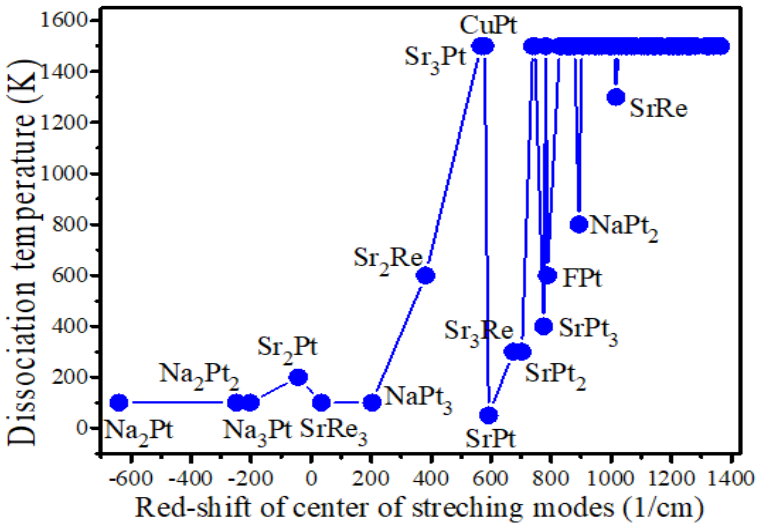

Figure 2. The dependence of the catalytic dissociation temperature of water on the red shift of the center of the v_1 and v_3 modes of H_2O on various clusters. The red shift of the center of the v_1 and v_3 modes of H_2O is relative to that of the negatively charged isolated H_2O. Blue circles represent catalysts.

As illustrated in Figure 2, while the red shift of the center of the stretching modes is an effective descriptor of catalytic reactivity in water, the origin of some exceptions remains unknown. A multitude of factors, including molecular orbitals in proximity to the Fermi level, tunneling, resonances, the zero-point energy (ZPE) effect, and electron spin polarization, among others, can influence the reactivity of water [36–38,48,49,54]. The following section will provide a detailed examination of the mechanism of catalytic water activation.

3.3. Resonant Absorption of Heat of Adsorption Versus Dissociation Temperature

Faradzhev *et al.* found that water dissociation on Ru(0 0 0 1) can be achieved by thermal or by electronic excitation [50]. Therefore, charge transfer, adsorption energy, bond length, frontier orbitals, and density of states were considered to elucidate the underlying mechanisms of catalytic water activation. In order to examine the relationship between the heat of reaction of adsorption of water molecules and the excitation of the electronic state, we combine the LUMO-HOMO gap (E_g) and the adsorption energy of H_2O (E_a). The adsorption energies of the water molecule on catalysts with high catalytic activity and several inactive catalysts, the LUMO-HOMO gaps of the catalysts adsorbing H_2O, and the corresponding dissociation temperature are listed in Table 2. From these data, it can be seen that lower dissociation temperatures always tend to correspond to systems where the sum of LUMO-HOMO gap and the adsorption energy of H_2O (E_g+E_a) is close to zero or the adsorption energy slightly higher than the LUMO-HOMO gap. If the exceptions are excluded, as in the cases of $SrRe_3$ and FPt, the dissociation temperature and the absolute values of E_g+E_a are strongly correlated in Table 2 with a Pearson correlation coefficient of 0.90. This means that if the heat released by the adsorption of H_2O is equal to or slightly greater than the energy required to excite an electron from the HOMO to the LUMO orbital, the catalytic water dissociation reaction will tend to occur. On the contrary, when the absolute value of (E_g+E_a) is greater than 0.25 eV, the reaction is generally difficult to occur. Accordingly, electronic state excitation triggered by resonant absorption of the heat of adsorption reaction is one of the important reasons for promoting the catalytic dissociation process of water molecules. This result is readily understandable when one considers that some scientists have observed that catalytic dissociation of water can be achieved on some metal substrates and oxide monolayers by providing energy corresponding to the lowest unoccupied molecular orbital (LUMO) energy of water [41,51–53]. Although the adsorption energy of water on Sr_2Re is slightly 0.05 eV lower than that of the LUMO-HOMO gap, the quantum tunneling effect may be contributing factors to the catalytic water dissociation reaction.

Preprints.org (www.preprints.org) | NOT PEER-REVIEWED | Posted: 18 February 2025 doi:10.20944/preprints202502.1433.v1

For the case of $SrRe_3$, it has the absolute value of (E_g+E_a) of 0.3 eV, but a low dissociation temperature of 100 K, which attributes to the Frontier molecular orbitals and will be discussed in Section 3.4. For FPt, the corresponding (E_g+E_a) value is 2.11 eV, which are considerably far from the resonance region, but with a dissociation temperature of 600 K. This is mainly due to the fact that the products of dissociation of water molecules on FPt are an H adsorbed on the Pt atom and a free HO group, which leads to the entropy from the intermediate state to the product is increased, that is, the entropy-driven effect plays an important role in this reaction. This is opposite to the entropy change in the dissociation reaction of water on other catalysts, as shown in Figure S1.

Table 2. Δ*IR* represents the redshift of the stretching mode center relative to negatively charged H_2O. E_g denotes the LUMO-HOMO gap, E_a is the adsorption energy, and T_d is the dissociation temperature.

Systems	Δ*IR* (1/cm)	E_g (eV)	E_a (eV)	E_a+E_g (eV)	T_d (K)
Na_2Pt	-640.5	0.71	-0.90	-0.19	100
Na_2Pt_2	-249.5	0.75	-0.97	-0.22	100
Na_3Pt	-203.1	0.67	-0.86	-0.19	100
Sr_2Pt	-42.8	0.60	-0.80	-0.20	200
$SrRe_3$	34.1	0.28	-0.58	-0.30	100
Sr_2Re	381.3	0.73	-0.68	0.05	600
CuPt	578.5	0.35	-1.02	-0.67	1500
SrPt	591.8	0.74	-0.76	-0.02	50
Sr_3Re	673.8	0.59	-0.68	-0.09	300
$SrPt_2$	702.0	0.96	-1.09	-0.13	300
Sr_2Pt_2	745.3	0.45	0.59	1.04	1500
$SrPt_3$	774.9	0.73	-0.98	-0.25	400
FPt	787.4	2.95	-0.84	2.11	600
$NaPt_2$	892.9	0.44	-1.01	-0.57	800
SrRe	1015.9	0.55	0.30	0.85	1300

The correlation between dissociation temperature and both (E_g+E_a) and Δ*IR* has been illustrated in Figure 3, thereby facilitating a more straightforward comprehension of this relationship. One can see that when the Δ*IR* of water molecules after adsorption is lower and the value of (E_g+E_a) within the range of 0 to -0.30 eV (between the two blue dashed lines), the corresponding catalytic dissociation temperature of water molecules is usually lower, as shown in Figure 3. It is in alignment with the conclusions presented in both sections 3.2 and 3.3.

Preprints.org (www.preprints.org) | NOT PEER-REVIEWED | Posted: 18 February 2025 doi:10.20944/preprints202502.1433.v1

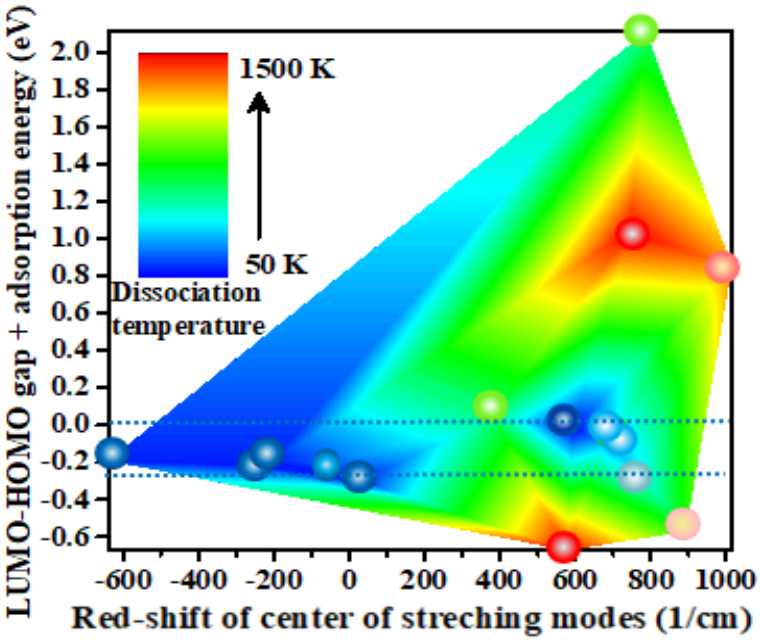

Figure 3. The dependence of dissociation temperature on (E_g+E_a) and the red shift of the centre of υ_1 and υ_3 modes of H_2O was plotted. The color of the ball is indicative of the dissociation temperature of H_2O on the corresponding catalyst.

3.4. The Function of the Frontier Molecular Orbitals (FMOs)

The concept of locality in physical space is of paramount importance in the understanding of the underlying mechanisms of chemical reactivity. Frontier molecular orbitals (FMOs) serve to identify the locality of chemical bonds that are chemically reactive, due to the associated orbital energies, and have thus far proven to be an invaluable tool in the description of chemical reactivity [*55*,*56*]. In order to gain a more comprehensive understanding of the reaction kinetics of water dissociation, a detailed analysis was performed of the frontier orbitals of the catalysts with adsorbed H_2O molecules and the frontier orbitals of the intermediate state in the catalytic dissociation reaction, as illustrated in Figure S1. By comparing the frontier orbitals of the reaction precursors and the intermediate states, it is possible to identify which orbitals play a role in the dissociation process. The configuration of the frontier orbitals (HOMO-1, HOMO, and LUMO) of precursors is essentially identical to that of the intermediate states in the reaction, which indicates that the frontier orbitals of reaction precursors play a pivotal role in the catalytic reaction process. In a few instances, the order of frontier orbits underwent a slight alteration. For instance, as illustrated in Figure S1, the energy hierarchy of the HOMO and LUMO of $SrReH_2O$ (precursor) underwent a reversal, with the energy levels of HOMO-1 and HOMO of Sr_2ReH_2O (precursor) shifting upwards to become the HOMO and LUMO of the intermediate state, respectively. A comparison of the frontier orbitals (HOMO-1, HOMO, and LUMO) of the precursor and intermediate state in the dissociation process reveals that the number of orbitals involved in the reaction process (orbitals from catalysts with increased overlap with H atoms during H_2O dissociation) is inversely proportional to the corresponding H_2O dissociation temperature. This is a logical conclusion, as the larger the overlap integral, the stronger the interaction between H and catalytic atoms will be. This phenomenon has been observed by Kawai and colleagues in their study of the role of molecular orbitals near the Fermi level in the excitation of vibrational modes of a single water molecule. In this study, a molecule is chemisorbed onto the metal surface, resulting in the formation of a molecule-metal bond and the rehybridization of the molecule's orbitals [57]. In Figure 4, we utilize CuPt, SrPt, and Sr_2Re as illustrative examples to elucidate the influence of frontier orbitals on catalytic water dissociation reactions. For CuPt, a comparison of the two sets of frontier orbitals on the left in Figure 4 reveals that only the LUMO orbitals are involved in the catalytic separation of H from H_2O molecules, without the assistance of resonance absorption. Consequently,

Preprints.org (www.preprints.org) | NOT PEER-REVIEWED | Posted: 18 February 2025 doi:10.20944/preprints202502.1433.v1

this material is unable to effectively catalyze the water dissociation reaction at temperatures below 1500K. From an energetic standpoint, the HOMO-LUMO gap (E_g) and the heat generated by the adsorption of water molecules are nearly identical, which evidently satisfies the prerequisite for the resonance absorption in the case of SrPt. Furthermore, the incorporation of both the HOMO and LUMO orbitals into the process of H separation can be observed in the frontier orbitals of the intermediate state. Both of these processes result in lower dissociation temperatures on SrPt. In the case of Sr_2Re, as illustrated in the two sets of images on the right in Figure 4, the HOMO-1 and LUMO orbitals of the intermediate state participate in the catalytic process of H_2O decomposition through changing the level order, thus lowering the corresponding dissociation temperature compared to that on CuPt. Ditto for the dissociation of water molecules on $SrRe_3$ as shown in Figure S1(e), where the homo-1, homo and LUMO orbitals are all involved in the catalytic water dissociation reaction, and thus the corresponding dissociation temperatures are as low as 100 K under conditions away from the energy resonance.

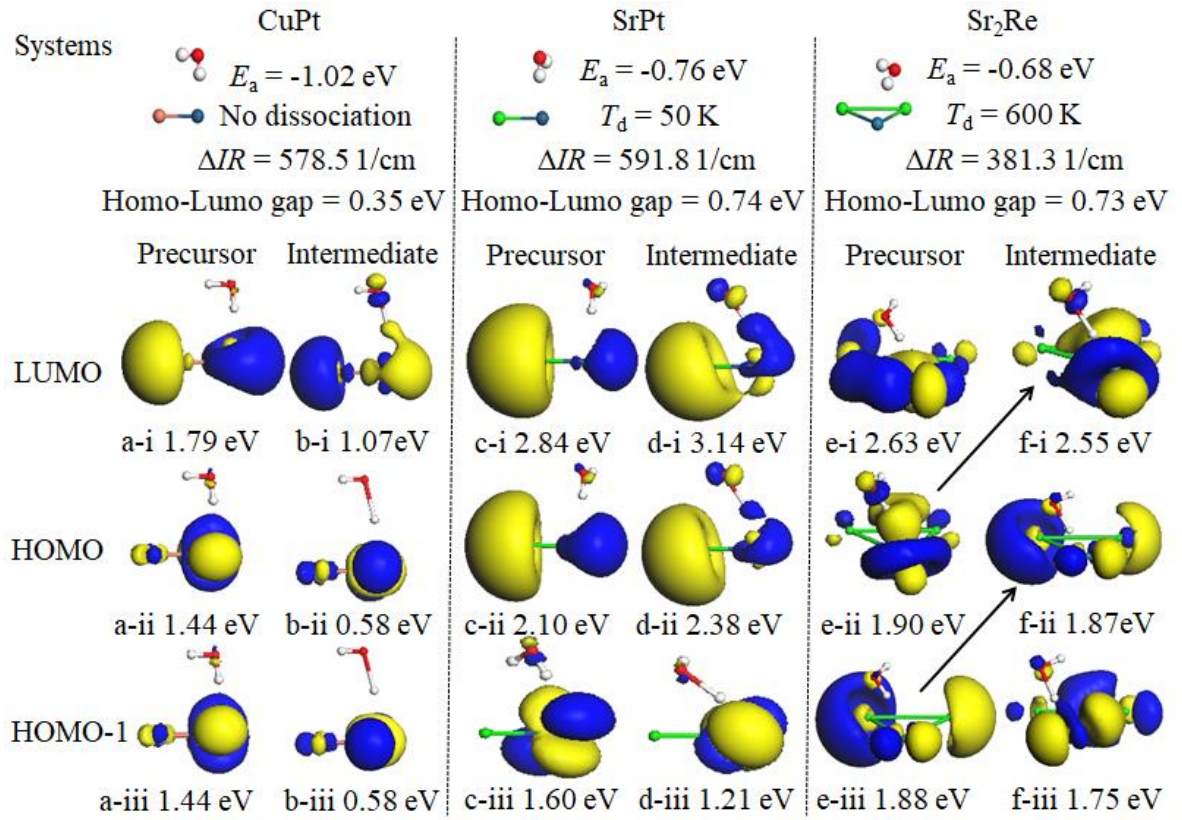

Figure 4. Frontier orbitals (HOMO-1, HOMO, and LUMO) of the precursors and intermediate states in the dissociation reaction for the examples of CuPt, SrPt, and Sr_2Re. E_a stands for adsorption energy of H_2O, ΔIR for red-shift of center of v_1 and v_3 modes of H_2O, T_d for dissociation temperature.

4. Conclusions

In conclusion, the redshift of the center of the v_1 and v_3 modes of H_2O (ΔIR) can reflect the catalytic activation of water molecules to a certain extent. However, a more profound comprehension of the activation mechanism of water molecules necessitates a comprehensive examination of the degree of involvement of the frontier orbitals and entropy changes. It is our conviction that these findings will stimulate further experimental and theoretical research in this domain.

Supplementary Materials: The following supporting information can be downloaded at the website of this paper posted on Preprints.org. Materials and Methods, Supplementary Text, Fig. S1.

Acknowledgments: The Natural Science Foundation of Jiangsu Province (Grant BK20150118), the Natural Science Foundation of Wuxi Institute of Technology (Grant ZK202104), the National Natural Science Foundation

Preprints.org (www.preprints.org) | NOT PEER-REVIEWED | Posted: 18 February 2025 doi:10.20944/preprints202502.1433.v1

of China (Grant 11905084), the Colleges and Universities in Jiangsu Province Natural Science Research Projects (Grant 20KJB140002) have provided financial support for this research, and Jiangsu University "Qing Lan Project" have also contributed to this endeavor.

Conflicts of interest: There are no conflicts of interest to declare.

Data and materials availability: All data are available in the main text or the supplementary materials.

References

1. Y. Li *et al.*, Recent Advances on Water-Splitting Electrocatalysis Mediated by Noble-Metal-Based Nanostructured Materials. *Adv. Energy Mater.* **10**, 1903120 (2020).
2. W. Yuan *et al.*, Visualizing H_2O Molecules Reacting at TiO_2 Active Sites with Transmission Electron Microscopy. *Science* **367**, 428–430 (2020).
3. H. Nishiyama *et al.*, Photocatalytic Solar Hydrogen Production from Water on a 100-m^2 Scale. *Nature* **598**, 304–307 (2021).
4. C. Kranz, M. Wächtler, Characterizing photocatalysts for water splitting: from atoms to bulk and from slow to ultrafast processes. *Chem. Soc. Rev.*, **50**, 1407–1437 (2021).
5. A. Fujishima, K. Honda, Electrochemical Photolysis of Water at a Semiconductor Electrode. *Nature*, **238**, 37–38 (1972).
6. T. Fujitani, I. Nakamura, A. Takahashi, H_2O Dissociation at the Perimeter Interface between Gold Nanoparticles and TiO_2 Is Crucial for Oxidation of CO. *ACS Catal.* **10**, 2517–2521 (2020).
7. J. L. C. Fajin, M. N. D. S. Cordeiro, F. Illas, J. R. B. Gomesc, Influence of step sites in the molecular mechanism of the water gas shift reaction catalyzed by copper. *J. Catal.* **268**, 131–141 (2009).
8. H. Prats, P. Gamallo, F. Illas, R. Sayós, Comparing the catalytic activity of the water gas shift reaction on Cu(321) and Cu(111) surfaces: Step sites do not always enhance the overall reactivity. *J. Catal.* **342**, 75–83 (2016).
9. S. C. Huang, C. H. Lin, J. H. Wang, Trends of Water Gas Shift Reaction on Close-Packed Transition Metal Surfaces. *J. Phys. Chem. C* **114**, 9826–9834 (2010).
10. F. Ahmad, M. K. Agusta, R. Maezono, H. K. Dipojono, DFT + U study of H_2O adsorption and dissociation on stoichiometric and nonstoichiometric CuO(111) surfaces. *J. Phys. Condens. Matter*. **32**, 045001 (2020).
11. N. A. Karim, M. S. Alias, S. K. Kamarudin, The Mechanism of the Water Dissociation and Dehydrogenation of Glycerol on Au(111) and PdAu Alloy Catalyst Surfaces. *Int. J. Hydrog. Energy* **46**, 30937-30947 (2021).
12. J. Wang *et al.*, Amorphization Activated Ruthenium-Tellurium Nanorods for Efficient Water Splitting. *Nat. Commun.* **10**, 5692 (2019).
13. J. L. C. Fajin, M. N. D. S. Cordeiro, F. Illas, J. R. B. Gomesc, Descriptors controlling the catalytic activity of metallic surfaces toward water splitting, *J. Catal.* **276**, 92–100 (2010).
14. R. Wu *et al.*, A Janus Nickel Cobalt Phosphide Catalyst for High-Efficiency Neutral-PH Water Splitting. *Angew. Chem. Int. Ed.* **47**, 15671-15675 (2018).
15. X. Zhang, Z. Feng, S. Zhang, Y. Liang, R. Wang, Engineering MoS_2 Basal Planes for Hydrogen Evolution via Synergistic Ruthenium Doping and Nanocarbon Hybridization. *Adv. Sci.* **6**, 1900090 (2019).
16. Y. Tang *et al.*, d-Band Center Modulating of CoO_x/Co_9S_8 by Oxygen Vacancies for Fast-Kinetics Pathway of Water Oxidation. *Chem. Eng. J.* **427**, 130915 (2022).
17. X. Miao *et al.*, Quadruple Perovskite Ruthenate as a Highly Efficient Catalyst for Acidic Water Oxidation. *Nat. Commun.* **10**, 3809 (2019).
18. T. Takata, K. Domen, Defect Engineering of Photocatalysts by Doping of Aliovalent Metal Cations for Efficient Water Splitting. *J. Phys. Chem. C* **113**, 19386–19388, (2009).
19. T. Takata, J. Jiang, Y. Sakata, M. Nakabayashi, K. Domen, Photocatalytic Water Splitting with a Quantum Efficiency of Almost Unity. *Nature* **581**, 411–414 (2020).
20. L. Mu *et al.*, Enhancing Charge Separation on High Symmetry $SrTiO_3$ Exposed with Anisotropic Facets for Photocatalytic Water Splitting. *Energy Environ. Sci.* **9**, 2463–2469 (2016).
21. Y. Zhang *et al.*, Single-atom Cu anchored catalysts for photocatalytic renewable H_2 production with a quantum efficiency of 56%. *Nat. Commun.* **13**, 58 (2022).

Preprints.org (www.preprints.org) | NOT PEER-REVIEWED | Posted: 18 February 2025 doi:10.20944/preprints202502.1433.v1

22. D. J. Haxton, T. N. Rescigno, C. W. McCurdy, Dissociative electron attachment to the H_2O molecule. II. Nuclear dynamics on coupled electronic surfaces within the local complex potential model. *Phys. Rev. A* **75**, 012711 (2007).
23. H. Adaniya *et al.*, Imaging the molecular dynamics of dissociative electron attachment to water. *Phys. Rev. Lett.* **103**, 233201 (2009).
24. B. Jiang, X. Ren, D. Xie, H. Guo, Enhancing dissociative chemisorption of H_2O on Cu(111) via vibrational excitation, PNAS, **109**, 10224–10227 (2012).
25. B. N. J. Persson, A. Baratoff, Inelastic electron tunneling from a metal tip: the contribution from resonant processes. *Phys. Rev. Lett.* **59**, 339–342 (1987).
26. C. C. Yu, K. Y. Chiang, M. Okuno *et al.*, Vibrational couplings and energy transfer pathways of water's bending mode. *Nat. Commun.* **11**, 5977 (2020).
27. T. Darling, D. M. Dennison, The Water Vapor Molecule. *Phys. Rev.* **57**, 128–139 (1940).
28. J. C. Polanyi, Concepts in reaction dynamics. *Acc. Chem. Res.* **5**, 161–168 (1972).
29. Y. Chang, F. An, Z. Chen *et al.* Vibrationally excited molecular hydrogen production from the water photochemistry. *Nat. Commun.* **12**, 6303 (2021).
30. F. F. Crim, State- and Bond-Selected Unimolecular Reactions. *Science* **249**, 1387 (1990).
31. F. F. Crim, Vibrational state control of bimolecular reactions: discovering and directing the chemistry. *Acc. Chem. Res.* **32**, 877 (1999).
32. B. Jiang, D. Xie, H. Guo, Vibrationally mediated bond selective dissociative chemisorption of HOD on Cu(111). *Chem. Sci.* **4**, 503-508 (2013).
33. A. Mondal, H. Seenivasan, A. K. Tiwari, Water dissociation on Cu (111): Effects of molecular orientation, rotation, and vibration on reactivity. *J. Chem. Phys.* **137**, 094708 (2012).
34. B. Jiang, J. Li, D. Xie, H. Guo, Effects of reactant internal excitation and orientation on dissociative chemisorption of H_2O on Cu(111): Quasi-seven-dimensional quantum dynamics on a refined potential energy surface. *J. Chem. Phys.* **138**, 044704 (2013).
35. H. Seenivasan, A. K. Tiwari, Water dissociation on Ni(100) and Ni(111): Effect of surface temperature on reactivity. *J. Chem. Phys.* **139**, 174707 (2013).
36. Z. Zhang, T. Liu, B. Fu, X. Yang, D. H. Zhang, First-Principles Quantum Dynamical Theory for the Dissociative Chemisorption of H_2O on Rigid Cu(111). *Nat. Commun.* **7**, 11953 (2016).
37. H. Seenivasan, B. Jackson, A. K. Tiwari, Water dissociation on Ni(100), Ni(110), and Ni(111) surfaces: Reaction path approach to mode selectivity. *J. Chem. Phys.* **146**, 074705 (2017).
38. S. Ghosh, D. Ray, A. K. Tiwari, Effects of alloying on mode-selectivity in H_2O dissociation on Cu/Ni bimetallic surfaces *J. Chem. Phys.* **150**, 114702 (2019).
39. P. M. Hundt, B. Jiang, M. E. van Reijzen, H. Guo, R. D. Beck, Vibrationally Promoted Dissociation of Water on Ni(111). *Science* **344**, 504–507 (2014).
40. B. Jiang, H. Guo, Control of mode/bond selectivity and product energy disposal by the transition state: X + H_2O (X = H, F, O(3P), and Cl) reactions. *J. Am. Chem. Soc.* **135**, 15251–15256 (2013).
41. B. Jiang, H. Guo, Relative efficacy of vibrational vs. translational excitation in promoting atom-diatom reactivity: Rigorous examination of Polanyi's rules and proposition of sudden vector projection (SVP) model. *J. Chem. Phys.* **138**, 234104 (2013).
42. H. J. Shin, J. Jung, K. Motobayashi *et al.*, State-selective dissociation of a single water molecule on an ultrathin MgO film. *Nature Mater.* **9**, 442–447 (2010).
43. M. Pavlo, G. Maxim, R. R. Thomas, V. B. Oleg, State-resolved spectroscopy of high vibrational levels of water up to the dissociative continuum. *Phil. Trans. R. Soc. A* **370**, 2710–2727, (2012).
44. Y. Wang, X. Zhang, G. Wu, Shift of Infrared Vibrational Spectra and H_2O Activation on PtCu Alloy Clusters. *AIP Adv.* **10**, 085019 (2020).
45. C. Qian, Y. Wang, Z. Wang, A DFT Study of Enhancement of H_2O Activation in Vibrational Excitation. *Inorganica Chim. Acta*. **514**, 119980 (2020).
46. J. P. Perdew, K. Burke, M. Ernzerhof, Generalized Gradient Approximation Made Simple. Generalized Gradient Approximation Made Simple. *Phys. Rev. Lett.* **77**, 3865-3868 (1996).
47. B. Delley, Hardness conserving semilocal pseudopotentials. *Phys. Rev. B* **66**, 155125 (2002).

Preprints.org (www.preprints.org) | NOT PEER-REVIEWED | Posted: 18 February 2025 doi:10.20944/preprints202502.1433.v1

48. T. Sun, Z. Tang, W. Zang *et al.* Ferromagnetic single-atom spin catalyst for boosting water splitting. *Nat. Nanotechnol.* **18**, 763–771 (2023).
49. W. Mtangi, V. Kiran, C. Fontanesi, R. Naaman, Role of the Electron Spin Polarization in Water Splitting. *J. Phys. Chem. Lett.* **6**, 4916–4922 (2015).
50. N. S. Faradzhev, K. L. Kostov, P. Feulner, T. E. Madey, D. Menzel, Stability of water monolayers on Ru(0 0 0 1): Thermal and electronically induced dissociation. Chemical Physics Letters **415**, 165-171 (2005).
51. L. J. Lauhon, W. Ho, Inducing and observing the abstraction of a single hydrogen atom in bimolecular reactions with a scanning tunneling microscope. J. *Phys. Chem. B* **105**, 3987–3992 (2001).
52. K. Morgenstern, K. H. Rieder, Dissociation of water molecules with the scanning tunnelling microscope. *Chem. Phys. Lett.* **358**, 250–256 (2002).
53. A. Mugarza, T. K. Shimizu, D. F. Ogletree, M. Salmeron, Chemical reaction of water molecules on Ru(0001) induced by selective excitation of vibrational modes. *Surf. Sci.* **603**, 2030–2036 (2009)
54. P. Maksyutenko, T. R. Rizzo, O. V. Boyarkin, A direct measurement of the dissociation energy of water. *J. Chem. Phys.* **125**, 181101 (2006).
55. J. Yu, N. Q. Su, W. Yang, Describing Chemical Reactivity with Frontier Molecular Orbitalets. *JACS Au* **2**, 1383−1394 (2022).
56. J. J. Browna, S. L. Cockroft, Aromatic reactivity revealed: beyond resonance theory and frontier orbitals. *Chem. Sci.* **4**, 1772-1780 (2013).
57. M. Ohara, Y. Kim, S. Yanagisawa, Y. Morikawa, M. Kawai, Role of Molecular Orbitals Near the Fermi Level in the Excitation of Vibrational Modes of a Single Molecule at a Scanning Tunneling Microscope Junction. *PRL* **100**, 136104 (2008).

Disclaimer/Publisher's Note: The statements, opinions and data contained in all publications are solely those of the individual author(s) and contributor(s) and not of MDPI and/or the editor(s). MDPI and/or the editor(s) disclaim responsibility for any injury to people or property resulting from any ideas, methods, instructions or products referred to in the content.